Agriculture and Food

AIMS Agriculture and Food, 7(3): 683–703.
DOI: 10.3934/agrfood.2022042
Received: 19 May 2022
Revised: 31 July 2022
Accepted: 02 August 2022
Published: 19 August 2022

http://www.aimspress.com/journal/agriculture

Research article

Spray-dryer feed preparation: Enzymatic degradation of glucomannan for iron nanoencapsulation

Dyah H Wardhani[1,*], Heri Cahyono[1], Hana N Ulya[1], Andri C Kumoro[1], Khairul Anam[2] and José Antonio Vázquez[3]

[1] Chemical Engineering Department, Universitas Diponegoro, Jl. Prof. Sudarto, SH, Tembalang, 50275, Indonesia
[2] Chemistry Department, Universitas Diponegoro, Jl. Prof. Sudarto, SH, Tembalang, 50275, Indonesia
[3] Instituto de Investigatións Mariñas (CSIC), Grupo de Reciclado y Valorización de Materiales Residuales (REVAL), r/ Eduardo Cabello, 6. Vigo, 36208. Galicia, Spain

* **Correspondence:** Email: dhwardhani@che.undip.ac.id; Tel: +62247460058.

Abstract: Viscosity of glucomannan (GM) needs to be modified to support its application for spray drying encapsulation. The purpose of this study was to investigate degradation of GM using cellulase that fulfills viscosity in a spray-dryer specification. This hydrolyzed glucomannan (HGM) was subsequently spray-dried for encapsulating iron. Lower initial GM concentrations (0.5–1%) reached approximately 0.30 Pa·s which allowed to be spray-dried after 100 min degradation using 10 mg/L cellulase. Meanwhile, viscosity of 1.5% and 1.7% GM did not reach the target viscosity even after 300 min. The n^{th}-order model was the most suitable model which fitted viscosity reduction of ⩽1.5% initial GM concentration (coefficient of determination, $R^2 > 0.98$), whereas the Mahammad model fitted the viscosity reduction of 1.75% initial GM concentration ($R^2 = 0.99$). Hydrolysis decreased the degree of polymerization and surface tension but increased the antioxidant activities of HGM. Smaller molecules of the polysaccharides were released after hydrolysis. Particles of encapsulated iron using HGM were more hydrophilic than those using GM. The iron tended to have a higher release rate at pH 6.8 than at pH 1.2 in the first 40 min. Hence, the HGM showed its ability to act as a control release matrix for the iron that needs a protection in the acid environment, and delivers them to the neutral site for absorption. Nanoencapsulation using 0.35 Pa·s viscosity of HGM was able to have 84% yield, 96.41% encapsulation efficiency, and 10% moisture content. Particle size of the iron encapsulation was dominated by 341.99 nm-diameter. This study shows a potency to use an appropriate viscosity of HGM

which not only allows to be spray-dried but also support in protecting the iron as aimed by encapsulation the iron. Performances and properties of this matrix on encapsulating other bioactive compounds become future study.

Keywords: cellulase; hydrolyzed glucomannan; enzymatic hydrolysis; iron encapsulation; spray-drying encapsulation; iron nanoparticles

1. Introduction

Iron is an important micronutrient for normal growth and proper human development. The iron (II) has better bioavailability and efficacy than the iron (III) [1]. Thus, it is important to protect the iron (II) from oxidation which leads to an unpleasant aroma and appearance [2]. Encapsulation had been developed through several methods to maintain efficacy and prevent degradation of active compounds. As one of the encapsulation method, spray drying preserves the bioactive material by quickly proceeds and obtains high encapsulation yield [3,4]. In addition, this method prevents thermal damage of the product due to long expose in high temperature [5]. Ribeiro et al. [6] demonstrated that phenolic compounds of an elderberry extract maintained their stability after 8 months of encapsulation using the spray drying method.

Performance of a spray drying product is affected by compatibility between matrix, active compounds and spray-dryer conditions. These conditions include but not limit to inlet gas temperature, matrix material type, active compound concentration, and matrix concentrations [7,8]. High viscosity of the matrix could block the nozzle spray and interrupt the drying process. Sosnik and Seremeta [9] reported that the maximum viscosity of the feed solution for Büchi Mini Spray Dryer B-290 is approximately 0.3 Pa·s. Yang et al. [10] found the highest yield of spray-dry encapsulation is produced using 0.2 Pa·s of feed viscosity. Commonly, lower viscosity of a matrix was obtained by using the low concentration. Dueik and Diosady [11] and Singh et al. [12] applied only 1%–1.5% chitosan for encapsulating iron using the spray drying method and obtained 75% as the highest yield. It was reported that viscosity of 1% medium molecular weight of chitosan reaches just above 0.2 Pa·s. In fact, Schoubben et al. [13] only used 0.4–0.8% alginate solution to obtain low viscosity feed (below 0.25 Pa·s) to prevent the strand formation.

Glucomannan (GM), a heteropolysaccharide composed of β-1,4-linked D-mannase and D-glucose, had been studied for encapsulating enzymes, cells, biological elements, and vitamins using various methods because of its bioavailability and stability [10]. Its high viscosity, which is up to 30 Pa·s for a 1% GM solution, has hindered its application as a spray drying encapsulant [14]. Considering GM's biodegradability and biocompatibility, adjusting GM viscosity to a suitable spray drying feed is necessary for broadening GM's applications. As the viscosity was affected by the length of polymeric chain, shorter glucomannan chain was expected for lower viscosity [15]. Attempts for decreasing the viscosity have been carried out using an acid, but they produced irritating side-products [16–18]. β-glucannase was used to hydrolyze GM for a cryoprotective effect on myofibrillar [19]. Wattanaprasert et al. [20] reduced the viscosity of 12% GM solution to 0.049 Pa·s using β-mannanase for 4 h for andrographolide spray-dry encapsulation. They also found an increase in yield and encapsulation efficiency after the enzymatic treatment. Cellulase was used by Yang et al. [10] to decrease the GM viscosity in sweet orange oil's spray-dry encapsulation. Moreover, hydrolysis has

been reported to improve antioxidant activity of hydrolyzed glucomannan (HGM) [21]. This antioxidant activity of HGM as an encapsulant also has a benefit on protecting sensitive active compounds from oxidation. However, reports on a kinetic model of GM degradation and its antioxidant activity development are limited. Efficacy and characteristics of the degraded GM as an encapsulation of spray-dried iron are also still rarely studied. It was expected that hydrolysis using cellulase allows to prepare suitable viscosity of HGM as spray-dryer feed for iron encapsulant which could protect this bioactive from the oxidation. Kinetic approach was applied to study viscosity profile during the hydrolysis. Physicochemical properties of the encapsulated iron were also observed. Hence, this study aimed to decrease GM viscosity enzymatically for spray-dryer feed and subsequently apply the low viscous GM for iron encapsulation.

2. Materials and method

2.1. Overview of experimental program

The experiment was conducted in 2 stages namely hydrolysis and spray drying, as displayed in Figure 1. HGM solution was prepared by hydrolyzing native GM solution using cellulase. After reached specific viscosity, iron was added to the solution, and spray dried it afterward to obtain the encapsulated iron powder. The analytical determinations were carried out on HGM and HGM-Fe powder.

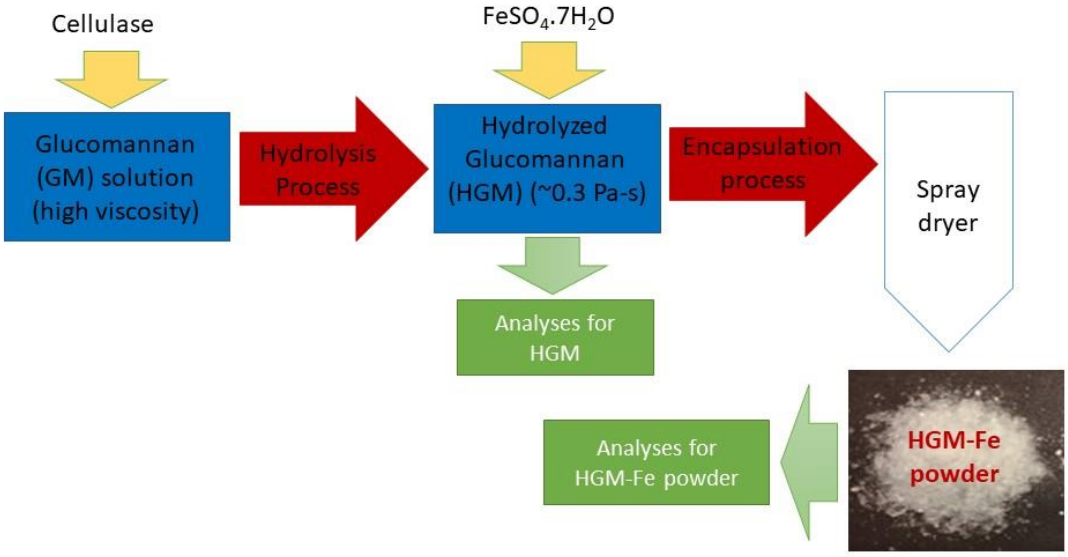

Figure 1. Schematic overview of experimental program.

2.2. Chemicals and reagents

The main material of this study was GM powder of Now Foods (Bloomingdale, Illinois, US) with weight average molecular weight (Mw) of 901,175 Da (determined by the GPC method in Section 2.4.2). Viscosity of 1% GM solution was 12.345 Pa·s. Cellulase enzyme of *Aspergillus niger* (Sigma-Aldrich,

St. Louis, Missouri, US) has activity of 0.3 U/mg, whereas ferrous sulfate heptahydrate ($FeSO_4 \cdot 7H_2O$) was obtained from Merck KgaA (Darmstadt, Hesse, Germany). Other chemicals were in analytical grade.

2.3. GM hydrolysis and spray dry of HGM-Fe

GM solution (1,000 mL) was hydrolyzed with cellulase (10 mg/L) under 350 rpm constant stirring using an overhead stirrer (Hightech Mixer RW 20 Digital, IKA, Staufen im Breisgau, Germany) at room temperature (~28 ℃). After 300 min, the hydrolysis was stopped by boiling the solution for 10 min to obtain HGM solution. Properties of the HGM solution was observed accordingly. The hydrolysis was conducted in various GM concentrations.

For iron encapsulation, HGM solution (500 mL) of 0.35 Pa·s was mixed with 68 mg of $FeSO_4 \cdot 7H_2O$ under continuous stirring for 15 min, followed by a spray drying process at 80 ℃ under a constant flow rate (1 mL/min). Characteristics of HGM-Fe as spray dried powder were determined.

2.4. Analytical determinations for HGM solution

2.4.1. Viscosity

Viscosity of each sample was measured using the Brookfield RVDV-II+Pro viscometer (AMETEK, Inc, Berwyn, Pennsylvania, US) at room temperature (~28 ℃) using spindle no. 2–7 at 100 rpm. Four mathematical models, i.e., order 1, order 2, order-n, and Mahammad (Eq (1)–(4), respectively) [22], were fitted to the viscosity reduction during hydrolysis for the kinetic study.

$$\eta = \eta_o e^{-kt} \tag{1}$$

$$\frac{1}{\eta} = \frac{1}{\eta_o} + kt \tag{2}$$

$$\eta = (\eta_o^{1-n} - (1-n)kt)^{\frac{1}{(1-n)}} \tag{3}$$

$$ln(\frac{\eta 0}{\eta}) = \frac{\alpha}{3} \times ln(1 + k't) \tag{4}$$

2.4.2. Average molecular weight

Molecular weight of samples was determined using two approaches, using Cannon Fenske Kapillar Viskometer, size 100 (Schott AG, Mainz, Rhineland-Palatinate, Germany) and gel permeation chromatography (GPC). The method base on Jin et al. [23] was applied for the viscometry approach. The intrinsic viscosity (η_{in}) of various concentrations of each sample solution (0.01, 0.02, 0.03, 0.04, and 0.05 g/L) was determined using the viscometer. Viscosity average molecular weight (Mv) was calculated from this viscosity using the Mark–Houwink equation for glucomannan (Eq (5)) [24].

$$\eta_{in} = 5.9610 \times 10^{-4}\, M^{0.7317} \tag{5}$$

Meanwhile, second approach in determining average molecular weight (Mw) and polydispersity

index (PDI) of GM and HGM were analyzed using The EcoSEC Elite® GPC System (Tosoh Bioscience LLC, King of Prussia, PA, USA) using THF as a solvent and polystyrene as molecular weight standards.

2.4.3. Degree of polymerization

Degree of polymerization (DP) was calculated from the ratio of total sugar (TS) and reducing sugar (RS) (Eq 6). TS was determined using the method of Do et al. [25]. The sample (2.0 mL) was mixed with a phenol solution (5%, 1.0 mL) and concentrated H_2SO_4 (98%, 5.0 mL) under boiling in a water bath for 15 min. The absorbance of the solution was read at 490 nm against glucose as a standard.

Meanwhile, the RS determination followed the method of Miller [26]. The sample (1.0 mL) was mixed with 3.0 mL of a 3,5-dinitrosalicylic acid (DNS) solution and boiled for 5 min. After being cooled down, the absorbance was measured at 550 nm. Glucose was used as a standard.

$$DP = \frac{TS}{RS} \tag{6}$$

2.4.4. Antioxidant activity

The scavenging activity of hydroxyl radicals was analyzed using the method of Yuan et al. [27] with slight modification. The sample (1.0 mL), phosphate buffer (0.4 mM, pH 7.4, 1.0 mL), 1,10-phenanthroline (2.5 mM, 1.0 mL), and H_2O_2 (20 mM, 0.5 mL) were mixed and incubated at 37 °C for 60 min. Absorbance of the solution was measured using a spectrophotometer at a 536 nm.

The analysis of DPPH radical scavenging activity was conducted following the method of Sun et al. [28]. Freshly prepared DPPH radical in a 95% ethanol solution (0.1 mM, 4.0 mL) was incubated with 4.0 mL of the sample for 30 min at room temperature (~28 °C) under a dark condition. The absorbance of the solution was then measured using a spectrophotometer at 517 nm.

2.4.5. Surface tension

Surface tension of native GM and HGM was determined using a Kruss K10T tensiometer (KARL KOLB GmbH & Co. KG, Dreieich, Hesse, Germany) at room temperature (~28 °C).

2.5. Analytical determination for HGM-Fe powder

2.5.1. Moisture content

The moisture content was determined using the AOAC Method [29] and calculated using Eq (7).

$$Moisture\ content(\%) = \frac{W_{sample} - W_{dried}}{W_{sample}} \times 100 \tag{7}$$

2.5.2. Encapsulation efficiency

The iron entrapped in the spray-dried HGM powder (0.1 g) was dissolved in a sodium citrate solution (100 mM, 20 mL). The solution was mixed with a phenanthroline solution (10 mL, 1.0 g/L), sodium acetate buffer (8.0 mL, 98.4 g/L), and a hydroxylamine hydrochloride solution (1.0 mL, 100 g/L) and then brought to 40 mL using distilled water. After 10 min, the absorbance of the solution was measured using a spectrophotometer at 508 nm against the iron standard. The encapsulation efficiency (EE) was calculated using Eq (8).

$$EE\ (\%) = \frac{Fe_{sample}}{Fe_{initially\ added}} \times 100\% \tag{8}$$

2.5.3. Swelling and solubility

The swelling and solubility of the sample was determined in 2 pH, i.e., pH 1.2 (HCl, 0.1 M) and pH 6.8 (buffer phosphate, 0.1 M) solutions [30]. The sample (0.1 g) was added to 100 mL of each pH solution, then heated at 60 ℃ for 30 min. After being cooled down, the sample was centrifuged to separate the supernatant and the pellet, both of which were subsequently oven-dried in different glass containers. The weight of the supernatant and pellet was measured before and after drying.

$$Solubility\ (\%) = \frac{weight\ of\ wet\ supernatant}{weight\ of\ dried\ supernatant} \times 100 \tag{9}$$

$$Swelling\ (\%) = \frac{weight\ of\ wet\ pellet}{weight\ of\ dried\ pellet} \times 100 \tag{10}$$

2.5.4. Water contact angle

For contact angle determination, the sample (0.5 g) was tableted (8 mm diameter). The contact angle was determined using a Contact Angle Meter (OCA 20, DataPhysics, Raiffeisenstraße, Filderstadt, Germany) at 25 ℃. A droplet of deionized water (3.0 μL) was deposited on the airside surface of the film (2.0 × 2.0 cm) using a precision syringe, and the contact angle was measured after 30 s of stabilization.

2.5.5. Iron release

Iron release from the encapsulation was observed by placing 0.1 g of the sample in an Erlenmeyer flask with 50 mL of the pH solution. Two pH solutions, i.e., pH 1.2 and pH 6.8 phosphate buffer (0.1 M) solutions, were used for the release determination. After shaking for a period of time, the filtrate was collected and examined for released iron.

2.5.6. Morphology and particle size

The morphology of the spray-dried particle was captured using an FEI Inspect S50 scanning electron microscope (ThermoFisher Scientific, Waltham, Massachusetts, United States) at 5 kV after the gold-coating process. The particle size distribution was observed using a laser diffraction

instrument (Malvern Mastersizer 2000, Malvern Panalytical Ltd., Worcestershire, UK).

2.5.7. Crystallinity

The crystallinity of the samples was determined using an Xpert Pro X-ray diffractometer (XRD, Malvern Panalytical, Malvern, Worcestershire, United Kingdom). The HGM-Fe powder samples were scanned at a rate of 5 min^{-1} in the range 10–90 ℃. The voltage and current of generator were set at 40 kV and 35 mA, respectively.

2.5.8. Infrared spectra

Infrared (IR) spectra of the samples were obtained using Perkin Elmer Spotlight 200 FTIR (PerkinElmer Inc., Waltham, MA, USA) at the range of 4,000–400 cm^{-1} wavenumber.

2.5.9. NMR spectroscopy

The ^{1}H NMR spectra of GM and HGM were recorded by JNM-ECZ500R NMR spectrometer (Jeol Ltd., Akishima, Japan) for 5 g/L sample concentration using D_2O as solvent. The analysis was conducted at room temperature (~28 ℃).

2.6. Statistical analysis

All experiments were carried out in triplicate, and the results are presented as means and standard deviations. Analysis of variance was conducted using Microsoft Excel 2019. The level of significance was set for $p < 0.05$.

3. Results and discussion

In this work, GM was enzymatically hydrolyzed to reduce the viscosity and was targeted for spray-dryer feed. High viscosity of native GM is not suitable for being sprayed and could block the nozzle of the spray-dryer. This work consisted of two stages, i.e., (i) GM hydrolysis for lowering the viscosity and (ii) spray dry of the HGM for encapsulating iron. Hydrolysis was conducted at various GM concentrations. Properties of this HGM were studied. The hydrolysis was targeted to obtain GM viscosity that would make GM suitable for being sprayed, around 0.3 Pa·s [9]. To predict the final viscosity target, decreasing of viscosity during hydrolysis was mathematically modelled using four models. The fittest model was applied to predict viscosity of HGM that is suitable for spraying. This appropriate HGM was subsequently applied as a matrix of iron encapsulation using the spray drying method.

3.1. Glucomannan hydrolysis

3.1.1. Viscosity

Initial viscosity dan the viscosity decrease profile of 0.5, 0.75, and 1.0% GM concentration

during 300 min hydrolysis showed an insignificant difference ($p > 0.05$) (Figure 2a). Meanwhile, initial viscosity of 1.5 and 1.75% GM solutions was approximately four and six times higher than that of 1% GM, respectively. A significant decrease of viscosity was observed in hydrolysis of various GM concentrations, in the first 60 min ($p < 0.05$), followed by a slight decline afterward. The highest concentration of GM (1.75%) showed the most drop of the viscosity than the other GM concentrations after 300 min, which decreased from 59.93 to 17.03 Pa·s. This suggested that the enzyme concentration was powerful to decrease the viscosity of the highest GM concentration, up to approximately 70%. After 300 min, viscosities of 1.5% and 1.75% substrates were still higher than those of the other substrate concentrations. Glucomannan is one of the polysaccharides with high viscosity. High concentration of dry matter formed higher initial viscosity in solution, which created empty space zone near the impeller and stagnant zones in other parts of the solution while mixing [31]. This inefficient mixing prevented the molecular contact between GM and the enzyme, and caused slower rate of viscosity degradation. A similar result was reported by Lu et al. [32] in enzymatic hydrolysis of a ball-milled corn stover.

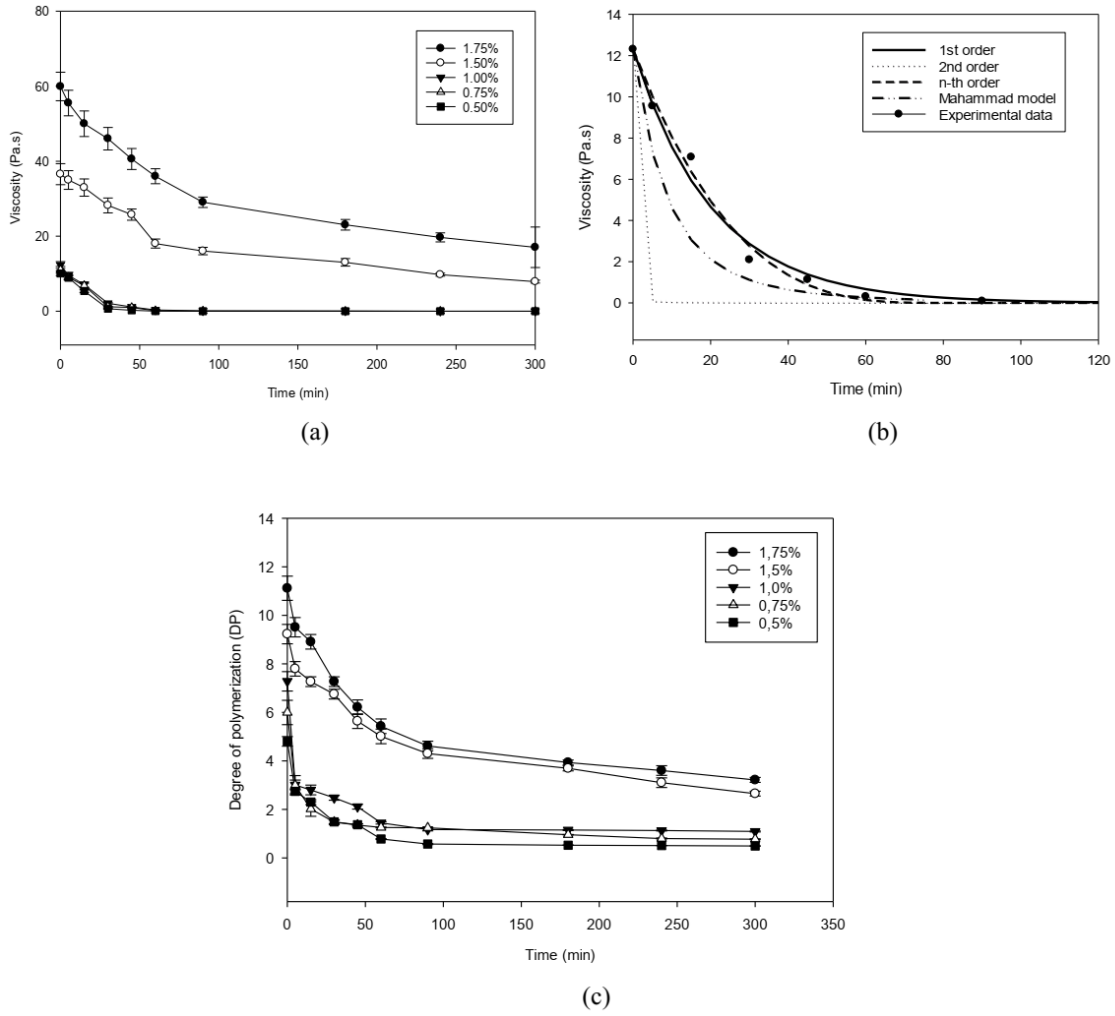

Figure 2. (a) The effect of initial GM concentrations on viscosity during hydrolysis ($p < 0.05$), (b) fitting of mathematical models on decreasing viscosity of 1% initial GM solution, and (c) the effect of initial GM concentrations on DP during hydrolysis.

Based on the result in Figure 2a, the viscosity target of approximately 0.3 Pa·s had been accomplished at 100 min for 0.5, 0.75, and 1% GM. Since the viscosity of a solution depends on its concentration, a longer duration of the hydrolysis process was needed for degrading a higher concentration of GM to achieve a desired viscosity level [33]. Since the hydrolysis was conducted in mild conditions and at a high-water content, longer than 5 h of hydrolysis should be avoided because of the possibility of bacterial contamination [34]. The contamination could interfere the hydrolysis by degrading the HGM obtained and releasing other compounds, such as acetic and lactic acids [35]. The initial GM concentrations indicated that the lower concentrations (0.5%–1%) enable to achieve the viscosity target over a shorter period. To obtain high yield of the spray-dry product, the 1% initial GM was subsequently used for iron encapsulation using the spray drying method. The viscosity value of the feed solution near the optimum point for spray drying was preferable because it prevented collisions between the wet droplets and the drying surface that increased the product yield [36].

Mathematical first order, second order, n^{th} order, and Mahammad models [22,37] were fitted to the viscosity data. The kinetic constants and the fitting model of each model are presented in Table 1 and Figure 1b, respectively. Based on the R^2 values, the n^{th} order was the best fit model to represent viscosity reduction of HGM of all initial GM concentrations, except in the highest GM concentration where the Mahammad model was the most fitted one. At higher GM concentrations, the length of the HGM chain could be more various after hydrolysis. The α of Mahammad's model was influenced by the temperature, intermolecular interactions, and polydispersity of the polymeric molecules and typically found at higher polymer concentration [22,38]. Hence, the Mahammad's model was less fit to describe the viscosity profile decrease at the low concentration of polymer concentration.

Table 1. Kinetic model of enzymatic hydrolysis of glucomannan.

[GM]	1st Order		2nd Order		nth Order			Mahammad model		
(%)	K (s^{-1})	R^2	k $((Pa{\cdot}s{\cdot}T)^{-1})$	R^2	K $((Pa{\cdot}s{\cdot}n^{-1}{\cdot}t)^{-1})$	n	R^2	α	k' (s^{-1})	R^2
0.50	0.0546	0.968	4.1719	0.741	0.2191	0.209	0.995	9.080	0.0866	0.882
0.75	0.0488	0.972	3.7064	0.845	0.1316	0.452	0.983	11.099	0.0401	0.942
1.00	0.0486	0.989	2.7926	0.697	0.0886	0.680	0.993	11.099	0.0305	0.922
1.50	0.0072	0.925	0.0003	0.979	0.0005	1.852	0.972	2.010	0.0246	0.966
1.75	0.0061	0.890	0.0001	0.982	0.0108	0.837	0.841	1.505	0.0328	0.989

3.1.2. Average molecular weight

The hydrolysis of GM produced GM oligosaccharides and reducing sugars that affected the molecular weight. The molecular weight of GM and HGM as the effect of hydrolysis was determined using 2 methods. Determination of Mv using Canon Fenske is presented in Table 2. After 300 min of hydrolysis, the most drop of Mv (87.52%) was obtained in the 0.5% GM solution. This result was in line with the viscosity result (Figure 2). The enzyme was effective in a low substrate concentration because the present active sites of the enzyme was sufficient to serve the GM low concentration. When a high substrate concentration was used, the active site of enzyme became saturated, thus lowering the hydrolysis rate. Moreover, higher concentration of GM led to produce thicker solution and formed gelation [39], which hindered the hydrolysis. As a result, the enzyme was less effective to cleavage the β,1-4 linkage of the highest GM concentration, and the Mv remained high even after 300 min.

Table 2. Viscosity average molecular weight (Mv) of HGM after 300 min hydrolysis using 10 mg/L cellulase ($p < 0.05$).

The concentration of GM (%)	Viscosity average molecular weight (Mv) HGM (Da)	Mv Decrease (%)
0.50	8,352 ± 21	87.52
0.75	11,982 ± 37	86.24
1.00	119,205 ± 16	84.14
1.50	288,016 ± 19	68.32
1.75	774,309 ± 20	60.89

Similar trend in molecular weight reduction was shown by GPC determination. The Mw of native GM decreased from 901,175 Da to 15,500 Da after hydrolysis for 300 min. A significant decrease was also observed in the number average molecular weight (Mn), from 33,889 Da to 11,792 Da. Although it had similar trend as found by the Canon Fenske method of Jin et al. [23], the GPC results obtained more precise result as it was not depended on solutions' viscosity and was also compared with standards. The polydispersity index (PDI), which measures molecular mass distribution was also determined. PDI which also called the heterogeneity index indicated the variety of macromolecules' chain length. Hydrolysis reduced PDI of GM from 26,592 to 1,314 for HGM. This result suggested that the hydrolysis has a tendency to form a more uniform chain length.

3.1.3. DP

GM is a polysaccharide consisting of two units of RS, i.e., glucose and mannose. Shorter polymer chain, showed by low DP value, supported the decrease of Mv caused by hydrolysis. During hydrolysis that cleaved the β-1,4 linkage of GM into oligosaccharides, the amount of RS increased, hence, reduced the DP as illustrated in Figure 2c. However, a higher concentration of GM formed a viscous solution that could inhibit molecular interaction with the enzymes and delayed the hydrolysis process. Slower hydrolysis in higher glucomannan concentration was also explained by Li et al. [40].

3.1.4. Antioxidant activity

An encapsulant that has antioxidant activity could support in protecting a sensitive bioactive compound from oxidation. Performance of HGM on a scavenging radical was determined using radicals of hydroxyl and DPPH that commonly reacted with biomacromolecules and was stable in room conditions [41,42]. Hydrolysis produced glucomannan oligosaccharides, which increased the inhibition activity and reduced IC_{50} as described in Figure 3a and b. The radicals interacted better with oligosaccharides than with polysaccharides through cell membrane transfer [43,44]. Higher GM concentrations produced more oligosaccharides that could act either donate their hydrogen or oxidize the radicals and scavenged more radicals [21,28]. IC_{50}, which shows the required dosage to 50% inhibition, was reduced after the hydrolysis. Benbettaïeb et al. [45] found that higher viscosity of solution had lower diffusivity coefficient and led to have less transfer contaminant through the viscous solution. This finding explained how the higher concentration of glucomannan had better inhibition activity, especially for 1.5 and 1.75% GM solution. Using β-mannanase, Liu et al. [21] reported a

positive correlation between scavenging activity of the hydroxyl radical and concentration of GM oligosaccharides. A similar antioxidant result was reported by Xiong et al. [46] on xanthan. Improvement of antioxidant capacity of HGM was beneficial in supporting HGM's application for inhibiting iron oxidation and protect changes of iron sensory and bioavailability [47].

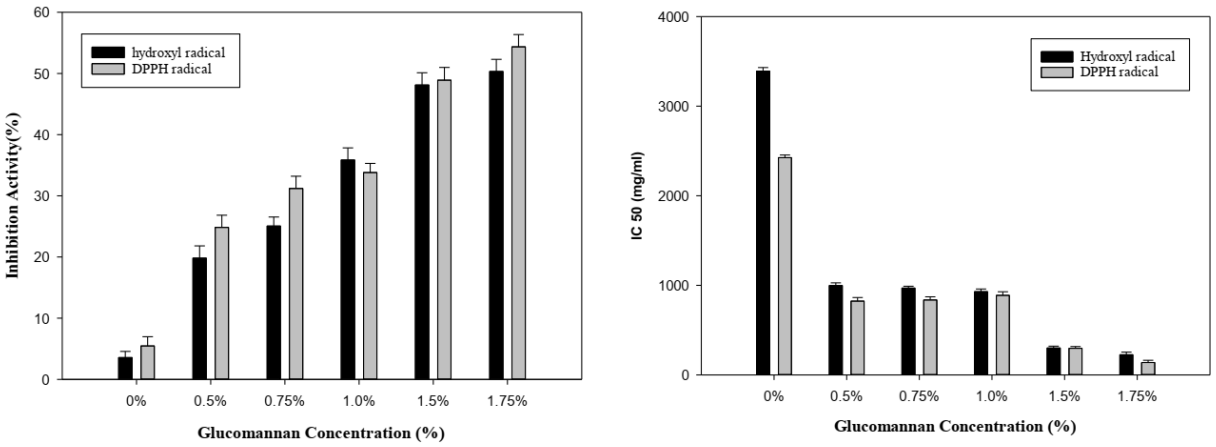

Figure 3. (a) The effect of GM concentration on HGM inhibitory activity and (b) the effect of GM concentration on IC50 HGM ($p < 0.05$).

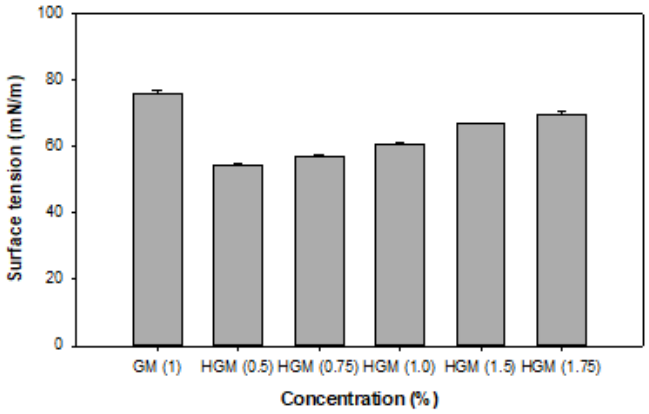

Figure 4. Surface tension of HGM ($p < 0.05$).

3.1.5. Glucomannan hydrophilicity

Figure 4 shows the hydrophilicity of HGM solutions from different substrate concentrations after 300 min of hydrolysis based on surface tension analysis. A higher value of surface tension indicated lower wettability, which led to hydrophobic properties [48]. Comparing to the native GM, lower surface tension was observed after hydrolysis of the lower GM concentration. This result suggested that a lower DP of GM oligosaccharides has a greater interaction with water than the cohesive forces associated with bulk water. This interaction was influenced by the primary molecular structure and viscosity [49]. HGM with a shorter polymer chain had better water absorption than GM [50]. Hence, the HGM of a lower GM concentration was appropriate for encapsulating hydrophilic

bioactive compounds such as the iron (II).

3.1.6. FTIR analysis

The IR spectra of the native and HGM of 0.35 Pa·s is shown in Figure 5. Hydroxyl groups are identified by the peak around 3,600–3,000 cm^{-1} wavenumber. The peaks at approximately 2,342 cm^{-1} and 2,091 cm^{-1} referred to the C=O bonds and C-H stretching bond, respectively. The effect of hydrolysis was insignificant on acetyl group spectra, as it appeared at 1,638–1,634 cm^{-1}. The glycosidic bond spectra of HGM appeared at lower intensity than those of GM (1,080–1,010 cm^{-1}), which suggested the occurrence of partial hydrolysis. The C-O-C pyranose ring of mannose and glucose was shown at the peak of 1,050 cm^{-1} [51]. The C-O-C vibration that referred to carbohydrate bonds was identified at 800–600 cm^{-1} [52]. This result showed a change in transmittance intensity of the same functional groups of GM after hydrolysis.

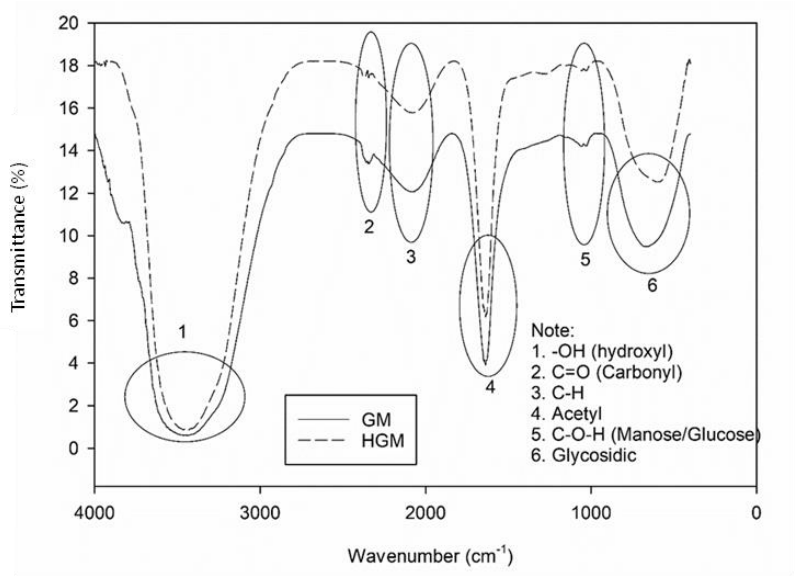

Figure 5. FTIR spectra comparison of GM and HGM.

3.1.7. ^{1}H NMR spectroscopy

The ^{1}H NMR spectra of native GM and HGM were shown at Figure 6. After hydrolysis, HGM showed higher intensity value at 5.26 and 4.67 ppm which identified as the chemical shift of H1 in the reducing end of glucoses. Signals between 4.7 and 4.8 ppm were also appeared as the H1 of the mannoses after glucomannan hydrolysis. The observed signals were similar to the NMR spectra of glucomannan found by Mikkelson et al. [53]. These results suggested that more oligosaccharide ends were produced after the cleavage of glucomannan polymer as the enzymatic hydrolysis applied.

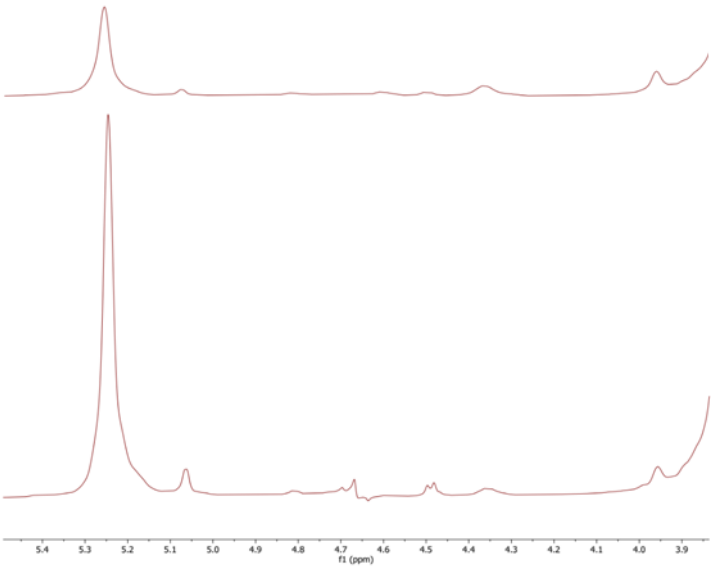

Figure 6. NMR spectra of GM (top) and HGM (bottom).

3.2. Characteristics of HGM-Fe encapsulation

HGM solution of 1% GM at a viscosity of 0.35 Pa·s was used as a matrix for iron encapsulation using spray drying method. Some characteristics of the HGM-Fe particle are shown in Table 3. The HGM-Fe encapsulation had 10% moisture content, lower than that in the report of Wardhani et al. [30], who found 14–17% using the same matrix. Although using similar viscosity of HGM, they used higher spray-dried temperatures (110–140 °C). Lower temperatures in our work permitted a lower drying rate and maximized water evaporation, thus resulting in lower moisture content. This value of moisture content cannot prevent the microbial growth, as it is higher that 5% [54]. GM hydrolysis produced lower molecular weight of polysaccharides, which increased its hygroscopicity and absorb more water content after powder formation [55]. However, Karn et al. [56] produced fortified curry powder with higher moisture content than 5%, which was relatively stable after 3 month storage. In fact, our moisture content result is lower than that of the Nepalese standard for powder storage, which is 14% [56].

Table 3. Characteristics of iron-encapsulation powders using 0.35 Pa·s HGM.

Parameter of iron encapsulated powders	Values
Water content (%)	10.07 ± 0.41
The efficiency of encapsulation (%)	96.41 ± 4.36
Yield (%)	84.00 ± 3.04
Swelling at pH 1.2 (%)	5.37 ± 0.37
Swelling at pH 6.8 (%)	4.79 ± 0.16
Solubility at pH 1.2 (%)	0.42 ± 0.56
Solubility at pH 6.8 (%)	1.92 ± 0.08

This spray drying method has 96% encapsulation efficiency, higher than that of the dropping method using deacetylated glucomannan, which is less than 70% [57]. The spray drying method allowed most of the solvent to be evaporated and left encapsulated the iron. Using acid HGM,

Guerreiro et al. [58] found that the efficiency ranged at 43%–104% and varied with the type of bioactive compound and the combined matrix. Meanwhile, Singh et al. [12] reported that the iron-encapsulation efficiency ranged at 85%–98% and varied with the matrix compound and its concentration.

Table 3 presents 84% yield of the spray-dried iron product using HGM. This yield was higher than the iron encapsulation obtained using chitosan and eudragit, as reported by Singh et al. [12]. Reducing HGM viscosity prior to the spray helped the encapsulant to be sprayed, thus increasing the yield. Moreover, many constituents contributed to performance of the spray drying process, including the spray drying parameters.

The swelling and solubility of iron particles were determined at acidic and neutral pH, which represent non-enzymatic human gastrointestinal conditions [59]. Swelling represented the increase of volume due to fluid absorption. Swelling of iron-loaded HGM encapsulation had an insignificant difference at both pH values ($p > 0.05$). Wu et al. [59] found that pH has no significant effect on the swelling of glucomannan because of the polysaccharide neutrality. Table 3 highlights that HGM-Fe powders have lower solubility in acid than in a neutral condition. This result suggested that HGM has a potency to protect iron release in acid solution, but release the iron in neutral solution.

The wettability of GM and iron-loaded HGM tablets was analyzed using the contact angle method as presented in Figure 7. The wettability properties have a strong correlation with solubility and release profile of a drug preparate [60]. The water contact angle value of GM- and HGM-loaded iron is 47.09° and 83.28°, respectively. Both of the results showed a value less than 90°, which indicates the hydrophilic characteristics. Lower MW and shorter sugar produced after hydrolysis could contribute to the increase of HGM hydrophilicity. This result was in line with the result discussed on the Section 3.1.5. A hydrophilic matrix is preferred to support the release control of the supplement [61].

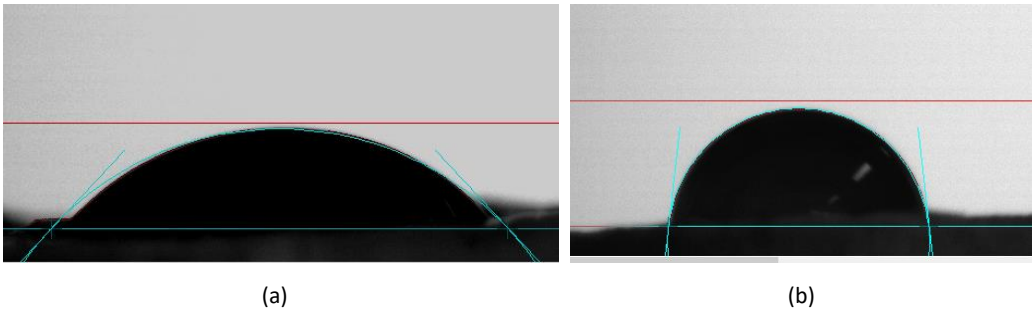

Figure 7. Water contact angle of tableted encapsulated iron using (a) HGM and (b) HGM-Fe.

The morphology of the HGM-Fe powders is presented in Figure 8a. The powders have round shape with several concave surfaces that could be due to uneven rate of drying between the surface and the core of the particle [9]. The particles have less surface cavity than the powders of Wardhani et al. [62], regardless of the fact that both studies used a HGM matrix. This could be due to lower spray-dry temperature of this study, which allowed a more uniform drying rate than that at higher temperature.

The bursting effect of iron from the HGM matrix was observed in the first 10 min of pH 6.8, followed by steadier iron release afterward until 60 min, as illustrated in Figure 8b. Meanwhile, a lower rate of iron release from the HGM matrix is shown at pH 1.2, but the release at pH 1.2 was comparable with that of pH 6.8 after 60 min. Figure 8b supports the result of the solubility of samples in different

pH as discussed in previous paragraph. This result suggested that HGM is a potential encapsulant for control release the iron that need a protection in the stomach environment, and deliver them to the duodenum for absorption [63]. A reverse trend was reported by Singh et al. [12] using chitosan and eudragit as encapsulants, where more iron release was found at lower pH solution. Various profile releases of iron from their encapsulant could be contributed due to different charges of the encapsulant.

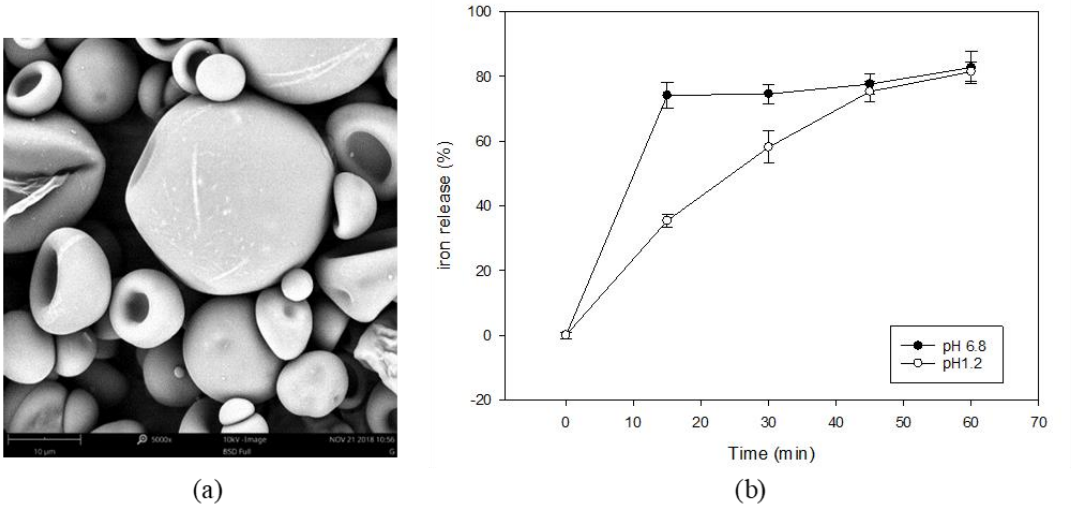

Figure 8. (a) Morphology of HGM-Fe powders at 5,000× magnifications and (b) Profile of iron release in buffer solutions at pH 1.2 and pH 6.8.

Particle size distribution of spray-dried HGM-Fe showed that nanoparticle size of powders ranged at 50.75–1718.47 nm, in which the highest percentage (12.11%) was dominated by the 341.99 nm size (Figure 9). At this size, the individual particle did not easy to be detected either visually or tongue-feel which supported its application as a fortificant. Moreover, this particle size was smaller than the spray-dried HGM of Wardhani et al. [62], who found 400–850 nm for spray drying at 110–140 ℃, and Guerreiro et al. [58], who obtained >1,300 nm particle sizes at 170 ℃ of spray drying. Using chitosan and eudragit in different concentrations as the iron matrix, Singh et al. [12] produced 0.5–5 μm iron particles at 150° of inlet spray drying. These discrepancies on particle size suggested that temperature, material of the matrix, and encapsulant concentration synergically contributed to the particle size. Our work conducted spray drying at 80 ℃, lower temperature than those used in the other works, which led to slower and more uniform drying rate. This allowed more water to be evaporated, thus producing smaller particles and lower moisture content.

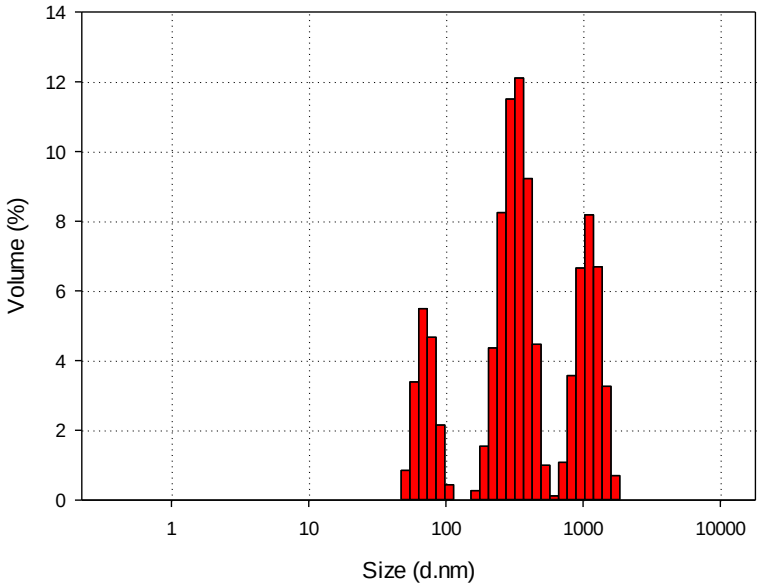

Figure 9. Particle size distribution of HGM-Fe.

Insignificant difference of crystallinity between GM and iron-loaded HGM was shown in the XRD patterns of both samples (Figure 10). A small amount of iron addition in the matrix solution did not change the crystallinity the HGM compared to that of GM native.

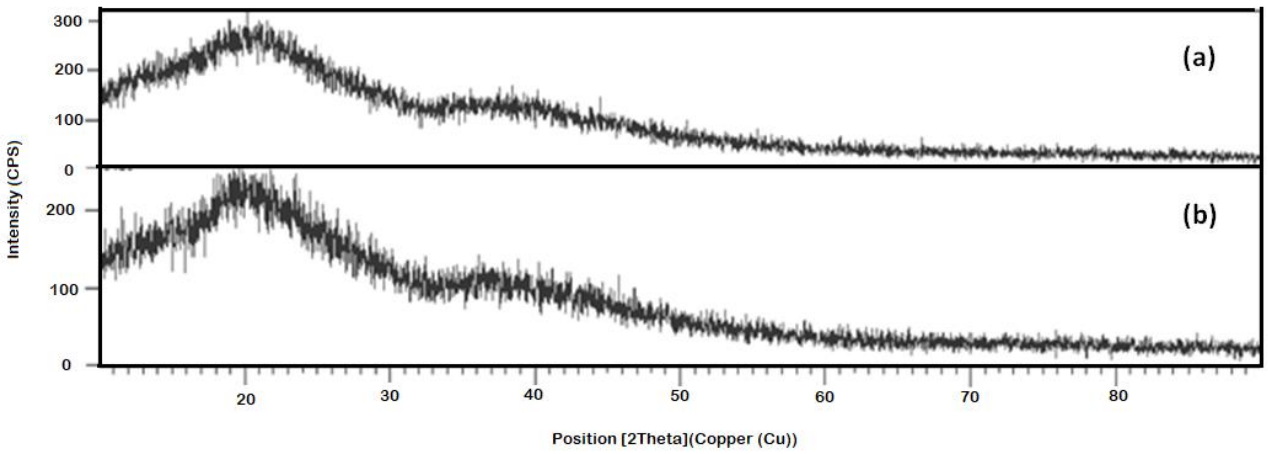

Figure 10. X-ray diffraction patterns; crystallinity of encapsulated iron using (a) GM and (b) HGM.

4. Conclusions

Hydrolysis of 1% GM using 10 mg/L cellulase for 100 min reduced the viscosity of HGM into 0.35 Pa·s, thus allowing the HGM to be spray-dried and used for iron encapsulant. The mathematical model of n^{th}-order kinetics was the best to represent the viscosity reduction of ≤1.5% initial GM concentration ($R^2 > 0.98$), whereas the Mahammad model well described the reduction of the higher initial GM concentration. Hydrolysis reduced surface tension of GM but led to improve antioxidant activities. Crystallinity and functional groups were insignificant change after hydrolysis followed by spray drying,

whereas the water contact angle tended to increase. Nanoencapsulation using a 0.35 Pa·s viscosity of HGM showed a 96.41% encapsulation efficiency, 10% moisture content and was dominated by a 341.99 nm particle size. HGM showed its ability to act as a control release matrix for the iron that need a protection in the acid environment, and deliver them to the neutral site for absorption. This study shows a potency to use an appropriate viscosity of HGM which not only allow to be spray-dried but also support to achieve the aims on encapsulating the iron.

Acknowledgments

This work was funded by Universitas Diponegoro through World Class Research Universitas Diponegoro (WCRU) scheme, 2021 (No. 118-14/UN.7.6.1/PP/2021).

Conflict of interest

The authors declare that they have no conflict of interest.

References

1. Santiago P (2012) Ferrous versus ferric oral iron formulations for the treatment of iron deficiency: A clinical overview. *Sci World J* 2012: 846824. https://doi.org/10.1100/2012/846824
2. Bryszewska MA (2019) Comparison study of iron bioaccessibility from dietary supplements and microencapsulated preparations. *Nutrients* 11: 273. https://doi.org/10.3390/nu11020273
3. Adamiec J, Borompichaichartkul C, Srzednicki G, et al. (2012) Microencapsulation of kaffir lime oil and its functional properties. *Dry Technol* 30: 914–920. https://doi.org/10.1080/07373937.2012.666777
4. Chong PH, Yusof YA, Aziz MG, et al. (2014) Effects of spray drying conditions of microencapsulation of Amaranthus gangeticus extract on drying behaviour. *Agric Agric Sci Proc* 2: 33–42. https://doi.org/10.1016/j.aaspro.2014.11.006
5. Costa SS, Machado BAS, Martin AR, et al. (2015) Drying by spray drying in the food industry: Micro-encapsulation, process parameters and main carriers used. *Afr J Food Sci* 9: 462–470. https://doi.org/10.5897/ajfs2015.1279
6. Ribeiro AM, Estevinho BN, Rocha F (2019) Spray drying encapsulation of elderberry extract and evaluating the release and stability of phenolic compounds in encapsulated powders. *Food Bioprocess Technol* 12: 1381–1394. https://doi.org/10.1007/s11947-019-02304-z
7. Marcela F, Lucía C, Esther F, et al. (2016) Microencapsulation of l-ascorbic acid by spray drying using sodium alginate as wall material. *J Encapsulation Adsorpt Sci* 6: 1–8. https://doi.org/10.4236/jeas.2016.61001
8. Tchabo W, Ma YK, Kaptso GK, et al. (2019) Process analysis of mulberry (*Morus alba*) leaf extract encapsulation: Effects of spray drying conditions on bioactive encapsulated powder quality. *Food Bioprocess Technol* 12: 122–146. https://doi.org/10.1007/s11947-018-2194-2
9. Sosnik A, Seremeta KP (2015) Advantages and challenges of the spray-drying technology for the production of pure drug particles and drug-loaded polymeric carriers. *Adv Colloid Interface Sci* 223: 40–54. https://doi.org/10.1016/j.cis.2015.05.003

10. Yang J, Xiao JX, Ding LZ (2009) An investigation into the application of konjac glucomannan as a flavor encapsulant. *Eur Food Res Technol* 229: 467–474. https://doi.org/10.1007/s00217-009-1084-2
11. Dueik V, Diosady LL (2017) Microencapsulation of iron in a reversed enteric coating using spray drying technology for double fortification of salt with iodine and iron. *J Food Process Eng* 40: e12376. https://doi.org/10.1111/jfpe.12376
12. Singh AP, Siddiqui J, Diosady LL (2018) Characterizing the pH-dependent release kinetics of food-grade spray drying encapsulated iron microcapsules for food fortification. *Food Bioprocess Technol* 11: 435–446. https://doi.org/10.1007/s11947-017-2022-0
13. Schoubben A, Blasi P, Giovagnoli S, et al. (2010) Development of a scalable procedure for fine calcium alginate particle preparation. *Chem Eng J* 160: 363–369. https://doi.org/10.1016/j.cej.2010.02.062
14. Tatirat O, Charoenrein S (2011) Physicochemical properties of konjac glucomannan extracted from konjac flour by a simple centrifugation process. *LWT-Food Sci Technol* 44: 2059–2063. https://doi.org/10.1016/j.lwt.2011.07.019
15. Bhaturiwala R, Bagban MA, Singh TA, et al. (2021) Partial purification and application of β-mannanase for the preparation of low molecular weight galacto and glucomannan. *Biocatal Agric Biotechnol* 36: 102155. https://doi.org/10.1016/j.bcab.2021.102155
16. Cheng LH, Nur Halawiah H, Lai BN, et al. (2010) Ultrasound mediated acid hydrolysis of konjac glucomannan. *Int Food Res J* 17: 1043–1050.
17. Ojima R, Makabe T, Prawitwong P, et al. (2009) Rheological property of hydrolyzed konjac glucomannan. *Trans Mater Res Soc Japan* 34: 477–480. https://doi.org/10.14723/tmrsj.34.477
18. Wang SH, Zhou B, Wang YT, et al. (2015) Preparation and characterization of konjac glucomannan microcrystals through acid hydrolysis. *Food Res Int* 67: 111–116. https://doi.org/10.1016/j.foodres.2014.11.008
19. Wang L, Xiong GQ, Peng YB, et al. (2014) The cryoprotective effect of different konjac glucomannan (KGM) hydrolysates on the glass carp (*Ctenopharyngodon idella*) myofibrillar during frozen storage. *Food Bioprocess Technol* 7: 3398–3406. https://doi.org/10.1007/s11947-014-1345-3
20. Wattanaprasert S, Borompichaichartkul C, Vaithanomsat P, et al. (2017) Konjac glucomannan hydrolysate: A potential natural coating material for bioactive compounds in spray drying encapsulation. *Eng Life Sci* 17: 145–152. https://doi.org/10.1002/elsc.201600016
21. Liu JH, Xu QH, Zhang JH, et al. (2015) Preparation, composition analysis and antioxidant activities of konjac oligo-glucomannan. *Carbohyd Polym* 130: 398–404. https://doi.org/10.1016/j.carbpol.2015.05.025
22. Mahammad S, Comfort DA, Kelly RM, et al. (2007) Rheological properties of guar galactomannan solutions during hydrolysis with galactomannanase and α-galactosidase enzyme mixtures. *Biomacromolecules* 8: 949–956. https://doi.org/10.1021/bm0608232
23. Jin WP, Mei T, Wang YT, et al. (2014) Synergistic degradation of konjac glucomannan by alkaline and thermal method. *Carbohyd Polym* 99: 270–277. https://doi.org/10.1016/j.carbpol.2013.08.029
24. Li B, Xie BJ (2004) Synthesis and characterization of konjac glucomannan/poly(vinyl alcohol) interpenetrating polymer networks. *J Appl Polym Sci* 93: 2775–2780. https://doi.org/10.1002/app.20769

25. Do BC, Dang TT, Berrin JG, et al. (2009) Cloning, expression in Pichia pastoris, and characterization of a thermostable GH5 mannan endo-1,4-beta-mannosidase from *Aspergillus niger* BK01. *Microb Cell Fact* 8: 59.
26. Miller GL (1959) Use of dinitrosalicylic acid reagent for determination of reducing sugar. *Anal Chem* 31: 426–428. https://doi.org/10.1021/ac60147a030
27. Yuan HM, Zhang WW, Li XG, et al. (2005) Preparation and in vitro antioxidant activity of κ-carrageenan oligosaccharides and their oversulfated, acetylated, and phosphorylated derivatives. *Carbohyd Res* 340: 685–692. https://doi.org/10.1016/j.carres.2004.12.026
28. Sun LN, Qian JG, Blough NV, et al. (2015) Insights into the photoproduction sites of hydroxyl radicals by dissolved organic matter in natural waters. *Environ Sci Technol Lett* 2: 352–356. https://doi.org/10.1021/acs.estlett.5b00294
29 AOAC (2005) Official Methods of Analysis of AOAC International.
30. Wardhani DH, Wardana IN, Ulya HN, et al. (2020) The effect of spray-drying inlet conditions on iron encapsulation using hydrolysed glucomannan as a matrix. *Food Bioprod Process* 123: 72–79. https://doi.org/10.1016/j.fbp.2020.05.013
31. Battista F, Bolzonella D (2018) Some critical aspects of the enzymatic hydrolysis at high dry-matter content: A review. *Biofuel Bioprod Biorefin* 12: 711–723. https://doi.org/10.1002/bbb.1883
32. Lu MS, Li JB, Han LJ, et al. (2020) High-solids enzymatic hydrolysis of ball-milled corn stover with reduced slurry viscosity and improved sugar yields. *Biotechnol Biofuels* 13: 77. https://doi.org/10.1186/s13068-020-01717-9
33. Pawlowski L (2009) Suspension and solution thermal spray coatings. *Surf Coat Tech* 203: 2807–2829. https://doi.org/10.1016/j.surfcoat.2009.03.005
34. Akesowan A (2012) Syneresis and texture stability of hydrogel complexes containing konjac flour over multiple freeze-thaw cycles. *Life Sci J* 9: 1363–1367.
35. Serate J, Xie D, Pohlmann E, et al. (2015) Controlling microbial contamination during hydrolysis of AFEX-pretreated corn stover and switchgrass: Effects on hydrolysate composition, microbial response and fermentation. *Biotechnol Biofuels* 8: 180. https://doi.org/ 10.1186/s13068-015-0356-2
36. Nambiar RB, Sellamuthu PS, Perumal AB (2017) Microencapsulation of tender coconut water by spray drying: effect of Moringa oleifera gum, maltodextrin concentrations, and inlet temperature on powder qualities. *Food Bioprocess Technol* 10: 1668–1684. https://doi.org/10.1007/s11947-017-1934-z
37. Tayal A, Pai VB, Khan SA (1999) Rheology and microstructural changes during enzymatic degradation of a guar-borax hydrogel. *Macromolecules* 32: 5567–5574. https://doi.org/10.1021/ma990167g
38. Nobile MR, Cocchini F (2000) Predictions of linear viscoelastic properties for polydisperse entangled polymers. *Rheol Acta* 39: 152–162. https://doi.org/10.1007/s003970050015
39. Zhang H, Yoshimura M, Nishinari K, et al. (2001) Gelation behaviour of konjac glucomannan with different molecular weights. *Biopolymers* 59: 38–50. https://doi.org/10.1002/1097-0282(200107)59:1<38::AID-BIP1004>3.0.CO;2-A
40. Li GJ, Qi L, Li AP, et al. (2004) Study on the kinetics for enzymatic degradation of a natural polysaccharide, *konjac glucomannan*. *Macromol Symp* 216: 165–178. https://doi.org/10.1002/masy.200451216
41. Xie JH, Shen MY, Xie MY, et al. (2012) Ultrasonic-assisted extraction, antimicrobial and antioxidant activities of Cyclocarya paliurus (Batal.) Iljinskaja polysaccharides. *Carbohyd Polym* 89: 177–184. https://doi.org/10.1016/j.carbpol.2012.02.068

42. Škrovánková S, Mišurcová L, Machů L (2012) Antioxidant activity and protecting health effects of common medicinal plants. *Adv Food Nutr Res* 67: 75–139. 10.1016/B978-0-12-394598-3.00003-4
43. Patel S, Goyal A (2011) Functional oligosaccharides: Production, properties and applications. *World J Microbiol Biotechnol* 27: 1119–1128. https://doi.org/10.1007/s11274-010-0558-5
44. Jian WJ, Chen YH, Wang LY, et al. (2018) Preparation and cellular protection against oxidation of Konjac oligosaccharides obtained by combination of γ-irradiation and enzymatic hydrolysis. *Food Res Int* 107: 93–101. https://doi.org/10.1016/j.foodres.2018.02.014
45. Nasreddine B, Mahfoudh R, Moundanga S, et al. (2020) Modeling of the release kinetics of phenolic acids embedded in gelatin/chitosan bioactive-packaging films: Influence of both water activity and viscosity of the food simulant on the film structure and antioxidant activity. *Int J Biol Macromol* 160: 780–794. https://doi.org/10.1016/j.ijbiomac.2020.05.199
46. Xiong XY, Li M, Xie J, et al. (2013) Antioxidant activity of xanthan oligosaccharides prepared by different degradation methods. *Carbohyd Polym* 92: 1166–1171. https://doi.org/10.1016/j.carbpol.2012.10.069
47. Susan Khosroyar (2012) Ferric–Saccharate capsulation with alginate coating using the emulsification method. *Afr J Microbiol Res* 6: 2455–2461.
48. Yuan YH, Lee TR (2013) Contact angle and wetting properties. In: *Surface science techniques*, 51: 3–34. https://doi.org/10.1007/978-3-642-34243-1_1
49. Jin TX, Liu C, Zhou M, et al. (2015) Crystallization, mechanical performance and hydrolytic degradation of poly(butylene succinate)/graphene oxide nanocomposites obtained via in situ polymerization. *Compos Part A-Appl Sci Manuf* 68: 193–201. https://doi.org/10.1016/j.compositesa.2014.09.025
50. Song L, Xie WC, Zhao YK, et al. (2019) Synthesis, antimicrobial, moisture absorption and retention activities of kojic acid-grafted konjac glucomannan oligosaccharides. *Polymers* 11: 1979. https://doi.org/10.3390/polym11121979
51. Wiercigroch E, Szafraniec E, Czamara K, et al. (2017) Raman and infrared spectroscopy of carbohydrates: A review. *Spectrochim. Acta-Part A Mol Biomol Spectrosc* 185: 317–335. https://doi.org/10.1016/j.saa.2017.05.045
52. Huang DM, Hsiao JK, Chen YC, et al. (2009) The promotion of human mesenchymal stem cell proliferation by superparamagnetic iron oxide nanoparticles. *Biomaterials* 30: 3645–3651. https://doi.org/10.1016/j.biomaterials.2009.03.032
53. Mikkelson A, Maaheimo H, Hakala TK (2013) Hydrolysis of konjac glucomannan by *Trichoderma reesei* mannanase and endoglucanases Cel7B and Cel5A for the production of glucomannooligosaccharides. *Carbohyd Res* 372: 60–68. https://doi.org/10.1016/j.carres.2013.02.012
54. Aziz MG, Yusof YA, Blanchard C, et al. (2018) Material properties and tableting of fruit powders. *Food Eng Rev* 10: 66–80. https://doi.org/10.1007/s12393-018-9175-0
55. Caparino OA, Tang J, Nindo CI, et al. (2012) Effect of drying methods on the physical properties and microstructures of mango (Philippine 'Carabao' var.) powder. *J Food Eng* 111: 135–148. https://doi.org/10.1016/j.jfoodeng.2012.01.010
56. Karn SK, Chavasit V, Kongkachuichai R, et al. (2011) Shelf stability, sensory qualities, and bioavailability of iron-fortified Nepalese curry powder. *Food Nutr Bull* 32: 13–22. https://doi.org/10.1177/156482651103200102

57. Wardhani DH, Nugroho F, Aryanti N, et al. (2018) Simultaneous effect of temperature and time of deacetylation on physicochemical properties of glucomannan. *ASEAN J Chem Eng* 18: 1–8.
58. Guerreiro F, Pontes JF, da Costa AMR, et al. (2019) Spray-drying of konjac glucomannan to produce microparticles for an application as antitubercular drug carriers. *Powder Technol* 342: 246–252. https://doi.org/10.1016/j.powtec.2018.09.068
59. Wu J, Deng X, Lin XY (2013) Swelling characteristics of konjac glucomannan superabsobent synthesized by radiation-induced graft copolymerization. *Radiat Phys Chem* 83: 90–97. https://doi.org/10.1016/j.radphyschem.2012.09.026
60. Sarifudin A, Soontaranon S, Peerapattana J, et al. (2020) Mechanical strength, structural and hydration properties of ethanol-treated starch tablets and their impact on the release of active ingredients. *Int J Biol Macromol* 149: 541–551. https://doi.org/10.1016/j.ijbiomac.2020.01.286
61. Sultanova Z, Kaleli G, Kabay G, et al. (2016) Controlled release of a hydrophilic drug from coaxially electrospun polycaprolactone nanofibers. *Int J Pharm* 505: 133–138. https://doi.org/10.1016/j.ijpharm.2016.03.032
62. Wardhani DH, Wardana IN, Ulya HN, et al. (2020) The effect of spray-drying inlet conditions on iron encapsulation using hydrolysed glucomannan as a matrix. *Food Bioprod Process* 123: 72–79. https://doi.org/10.1016/j.fbp.2020.05.013
63. Ems T, Lucia KS, Huecker MR (2021) *Biochemistry, iron absorption*. StatPearls.